Slow light based on plasmon-induced transparency in dual-ring resonator-coupled MDM waveguide system

2014 J. Phys. D: Appl. Phys. 47 205101

(http://iopscience.iop.org/0022-3727/47/20/205101)

IOP Publishing Journal of Physics D: Applied Physics
J. Phys. D: Appl. Phys. **47** (2014) 205101 (6pp) doi:10.1088/0022-3727/47/20/205101

Slow light based on plasmon-induced transparency in dual-ring resonator-coupled MDM waveguide system

Shiping Zhan[1], Hongjian Li[1,2], Guangtao Cao[2], Zhihui He[1], Boxun Li[1] and Hui Yang[1]

[1] College of Physics and Electronic, Central South University, Changsha 410083, People's Republic of China
[2] College of Materials Science and Engineering, Central South University, Changsha 410083, People's Republic of China

E-mail: lihj398@csu.edu.cn

Received 21 December 2013
Accepted for publication 21 March 2014
Published 29 April 2014

Abstract

We report a theoretical and numerical investigation of the plasmon-induced transparency (PIT) effect in a dual-ring resonator-coupled metal–dielectric–metal waveguide system. A transfer matrix method (TMM) is introduced to analyse the transmission and dispersion properties in the transparency window. A tunable PIT is realized in a constant separation design. The phase dispersion and slow-light effect are discussed in both the resonance and non-resonance conditions. Finally, a propagation constant based on the TMM is derived for the periodic system. It is found that the group index in the transparency window of the proposed structure can be easily tuned by the period p, which provides a new understanding, and a group index ~51 is achieved. The quality factor of resonators can also be effective in adjusting the dispersion relation. These observations could be helpful to fundamental research and applications for integrated plasmonic devices.

Keywords: waveguide, optical resonators, surface plasmon, plasmonics

(Some figures may appear in colour only in the online journal)

1. Introduction

Electromagnetically induced transparency (EIT) is the result of a quantum destructive interference in a three-level atomic system [1, 2]. However, investigations on EIT are severely limited by the demanding conditions. Recent studies have revealed that the analogue in a classical system can be a novel way of understanding the quantum EIT due to the similar interference effects, mostly focusing on metamaterials [3–5], photonic crystals [6] and gratings [7]. A metal–dielectric–metal (MDM) waveguide, which supports the propagation of surface plasmon polaritons (SPPs) in the metal–dielectric interface and manipulating light on a subwavelength scale, can be regarded as an ideal optical element in an integrated plasmonic device [8, 9]. The plasmon-induced transparency (PIT), a plasmonic analogue of EIT, has been reported in a resonator-coupled MDM waveguide system [10–12]. Moreover, similarly to the quantum EIT, the slowed-down group velocity can also be found in the transparency window [12, 13]. For instance, Huang *et al* reported a slow-light effect in a stub-coupled MDM waveguide system, where a direct coupling can be noticed [12]. However, reports on the tunable dispersion properties based on indirect coupling are still infrequent. Meanwhile, the common understanding of a PIT with indirect coupling is attributed to the phase coupling, which usually is achieved by varying the separation between resonators [14, 15]. In order to meet the requirement of compact size for an integrated plasmonic device, tuning of the PIT in a constant separation rather than a varied one could be more convenient and guarantee a wider application. In addition, the existing research methods for a coupled MDM waveguide system are mainly presented as transmission

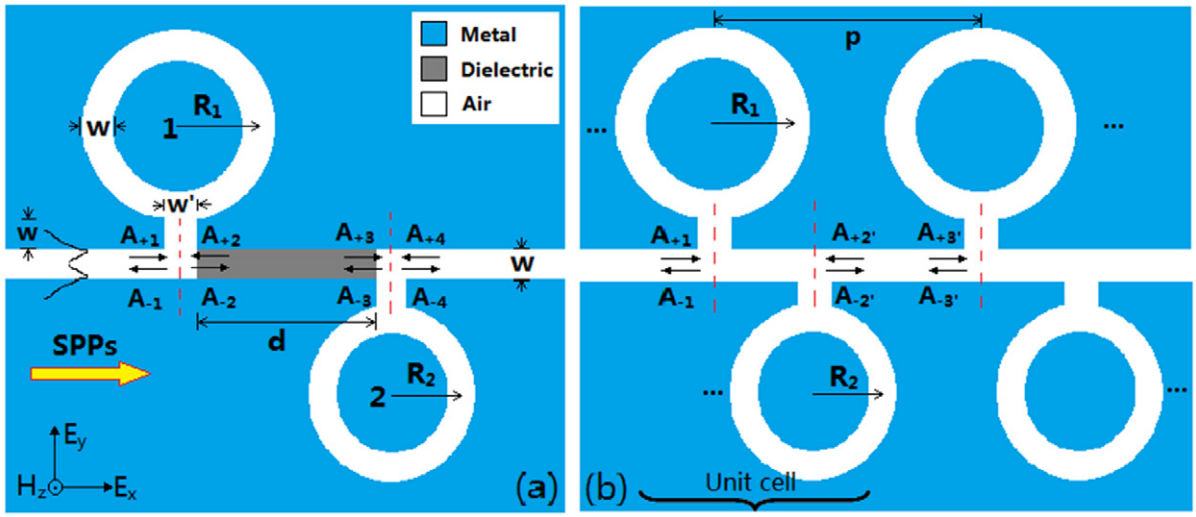

Figure 1. (*a*) A schematic diagram of the proposed MDM waveguide system. (*b*) The periodic system with the unit cell in (*a*) and period p.

line theory [16, 17], scattering theory [18] and coupled-mode theory (CMT [19, 20]). Here we introduce a CMT-based transfer matrix method (TMM) due to the fact that it can provide a clear understanding in dealing with the interaction between the two resonators, which is similar to the Fabry–Perot resonance in physics.

In this paper, the PIT effect in a dual-ring resonator-coupled MDM waveguide system is investigated theoretically and numerically. A CMT-based TMM is introduced for the theoretical fitting. We find that tuning of the PIT can be realized with a constant separation rather than a conventional varied one. The phase dispersion in the transparency window is found to be deeper in resonance and leads to a higher group index. Finally, the derived dispersion relation in the periodic system reveals that the group index n_g can be tuned by period p but in a different way, and a high $n_g \sim 51$ is achieved. We also find that the quality factor (QF) of resonators can be useful in tuning the dispersion property. The proposed configuration can be helpful to the fundamental research and applications for integrated plasmonic devices.

2. Structure and simulation

Figure 1(*a*) shows a schematic diagram of the proposed MDM waveguide system. Two aperture-coupled plasmonic ring resonators with a certain separation are placed in the opposite sides of the bus waveguide in which the SPPs may be formed when an incident pulse is input. The propagating SPP wave, which is confined in the metal–dielectric interface, may couple into the resonators due to the wave factor match and resonance condition [21]. In our proposed structure, a dielectric coloured grey with length d and permittivity ε_d is embedded in the bus waveguide between the two resonators, and w is the width for both bus waveguide and ring resonators. The aperture for each ring has length w and width w'. R_1 and R_2 are the effective radii for rings 1 and 2, respectively. The red dashed line represents the reference plane. The background metal is chosen to be silver (Ag), of which the frequency-dependent complex permittivity ε_m is approximated and defined by the Drude model [22] as

$$\varepsilon_m(\omega) = 1 - \frac{\omega_p^2}{\omega^2 + \gamma_p^2} + i\frac{\omega_p^2 \gamma_p^2}{\omega(\omega^2 + \gamma_p^2)}, \tag{1}$$

where ω stands for the angular frequency of the incident wave, $\omega_p = 1.38 \times 10^{16}\ s^{-1}$ is the bulk plasmon frequency, and $\gamma_p = 2.73 \times 10^{13}\ s^{-1}$ represents the damping rate, which characterizes the absorption loss. These values are obtained by fitting the experimental results [22]. The part coloured in white is chosen to be air with permittivity $\varepsilon_a = 1$ for simplicity. The characteristic spectral responses of the structures are found using the two-dimensional finite-difference time-domain (FDTD) method [23]. The spatial and temporal steps are set as $\Delta x = \Delta y = 2.5$ nm and $\Delta t = \Delta x/2c$ (c is the velocity of light in vacuum).

3. Theoretical and numerical discussion

3.1. PIT in two-ring coupled MDM system

We first deduced the related CMT-based TMM for analysing the spectral response. As depicted in figure 1(*a*), where $A_{\pm(2n-1)}$ and $A_{\pm 2n}(n = 1, 2)$ represent the energy amplitudes of input and output waves in the bus waveguide, respectively. According to the temporal CMT, the stable state of the two resonators can be described by a harmonic oscillator model as follows:

$$-i\omega a_n = (-i\omega_n - \frac{1}{\tau_{on}} - \frac{1}{\tau_{en}})a_1 + \sqrt{\frac{1}{\tau_{en}}}(A_{+(2n-1)} + A_{+2n}), \tag{2}$$

$$A_{-(2n-1)} = A_{+2n} - \sqrt{\frac{1}{\tau_{en}}}a_n, \quad A_{-2n} = A_{+(2n-1)} - \sqrt{\frac{1}{\tau_{en}}}a_n, \quad (n = 1, 2), \tag{3}$$

where a_n represents the mode amplitude of the nth resonator. ω is the angular frequency of the input optical pulse, $\omega_n(\lambda_n)$ is the

resonant frequency (wavelength) of the nth resonator, where $1/\tau_{on} = \gamma_{on} = \pi c/(\lambda_n Q_{on})$ and $1/\tau_{en} = \gamma_{en} = \pi c/(\lambda_n Q_{en})$ are the decay rates corresponding to the internal loss and the coupling loss to the waveguide, respectively. Q_{on} and Q_{en} are the related QFs which characterize the internal and the coupling loss. The relationship among Q_{tn}, Q_{on} and Q_{en} can be given as $1/Q_{tn} = 1/Q_{on} + 1/Q_{en}$, where Q_{tn} is the total QF of the nth single ring resonator in the coupling system and can be estimated as $Q_{tn} = \lambda_n/\delta\lambda_n$, and $\delta\lambda_n$ corresponds to the full-width at half-maximum (FWHM) of the transmission spectra. Q_{on} is the intrinsic QF and can be obtained from [24].

For the single ring resonator-coupled waveguide, due to the fact that the optical pulse is only inputted from the left port of the MDM waveguide, which means A_{+2} and A_{+4} are equal to zero. Hence the complex transmission t_n and reflection coefficient r_n can be derived from equations (2) and (3) as follows:

$$t_n = (\mathrm{i}(\omega_n - \omega) + \gamma_{on})/(\mathrm{i}(\omega_n - \omega) + \gamma_n), \tag{4a}$$

$$r_n = -\gamma_{en}/(\mathrm{i}(\omega_n - \omega) + \gamma_n), \quad (n = 1, 2), \tag{4b}$$

where $\gamma_n = \gamma_{on} + \gamma_{en}$.

The complex wave vector k_{MDM} of the SPPs in a MDM waveguide with width w can be given as in [10, 25], then the effective refractive index n_{eff} can be expressed as

$$n_{\mathrm{eff}} = \frac{k_{\mathrm{MDM}}}{k_0} = \sqrt{\varepsilon_{\mathrm{d}} - 2\varepsilon_{\mathrm{d}}\sqrt{\varepsilon_{\mathrm{d}} - \varepsilon_{\mathrm{m}}}/(k_0 w \varepsilon_{\mathrm{m}})}, \tag{5}$$

where $k_0 = 2\pi/\lambda$ is the wave vector in free space; ε_{d} and ε_{m} are permittivities for dielectric and metal, respectively. The total phase shift φ and loss factor ψ between resonators 1 and 2 can be given by

$$\begin{aligned} \varphi &= [2\pi(\mathrm{Re}(n_{\mathrm{eff}1})d + \mathrm{Re}(n_{\mathrm{eff}2})w')]/\lambda, \\ \psi &= [2\pi(\mathrm{Im}(n_{\mathrm{eff}1})d + \mathrm{Im}(n_{\mathrm{eff}2})w')]/\lambda, \end{aligned} \tag{6}$$

where the first terms in both φ and ψ relate to the MDM waveguide with length d and refractive index $n_{\mathrm{eff}1}$, while the second terms relate to the metal–air–metal waveguide with length w' and refractive index $n_{\mathrm{eff}2}$.

Then the relation between $A_{\pm2}$ and $A_{\pm3}$ can be expressed as $A_{+2} = A_{-3}\mathrm{e}^{\psi+\mathrm{i}\varphi}$, $A_{+3} = A_{-2}\mathrm{e}^{\psi+\mathrm{i}\varphi}$. Therefore, the input and output wave amplitudes of the whole system can be derived from the above analysis by a CMT-based TMM as

$$\begin{pmatrix} -\frac{r_1}{t_1 t_2}\mathrm{e}^{-h} & \frac{1}{t_1 t_2}\mathrm{e}^{-h} - \frac{r_1 r_2}{t_1 t_2}\mathrm{e}^{h} \\ -\frac{r_2}{t_2}\left(\frac{r_1}{t_1} + 1\right)\mathrm{e}^{h} & \frac{r_2}{t_1 t_2}\mathrm{e}^{-h} \\ -\frac{r_1 r_2}{t_1 t_2}\mathrm{e}^{-h} + \left(\frac{r_1}{t_1} + 1\right)\left(\frac{r_2}{t_2} + 1\right)\mathrm{e}^{h} & \\ +\frac{r_1}{t_1}\left(\frac{r_2}{t_2} + 1\right)\mathrm{e}^{h} & \end{pmatrix} \times \begin{pmatrix} A_{+1} \\ A_{-1} \end{pmatrix} = \begin{pmatrix} A_{+4} \\ A_{-4} \end{pmatrix}, \tag{7}$$

where we make $h = \psi + \mathrm{i}\varphi$ for conciseness and $t_n(r_n)$ is the transmission (reflection) coefficient given in equations (4a) and (4b). So the power transmission spectra of the coupled system can be calculated as

$$T = \left|\frac{A_{-4}}{A_{+1}}\right|^2 = \left|\frac{t_1 t_2}{1 - r_1 r_2 \mathrm{e}^{2(\psi+\mathrm{i}\varphi)}}\right|^2. \tag{8}$$

To verify the theoretical analysis above, both the simulative and theoretical transmission spectra for the structure of figure 1(a) with different permittivities ε_{d} are plotted, shown as figures 2(a)–(e), where radii R_1 and R_2 are set to be 174 nm and 171 nm, respectively, and other parameters are w = 50 nm, w' = 30 nm and d = 250 nm as a constant length. A typical EIT-like feature is observed in the transmission spectra, where a transparency peak at 736.4 nm is located between two dips at 723 and 747 nm [2]. We can see that as ε_{d} increases from 1 to 2 the maximum transmission of the transparency window shows a decreasing trend; however, it increases when ε_{d} achieves 2.9. The blue circles represent the theoretical results, which are in good agreement with the FDTD results, marked as a red solid line. The related QFs $Q_{\mathrm{t}1(2)}$ for ring 1 (2) are estimated at 73.2 (76.1), 140.7 (65.8), 57.5 (65.8), 31.7 (63) and 51.2 (71) when ε_{d} is varied from 1.0 to 2.9, while the corresponding $Q_{\mathrm{o}1(2)}$ is 372 (362) during the theoretical fitting. By further increasing ε_{d} to 3.2, the transmission maximum in the transparency window increases accordingly, and the relation between the transmission maximum and ε_{d} is shown in figure 2(f), where a non-monotonic trend is observed, which is similar to the realization of PIT by changing the separation [15]. This provides a convenient tuning of PIT in a constant separation, which may guarantee a wider application in integrated plasmonic devices. Figure 2(g) is the evolution of transmission phase shift θ with ε_{d}, where $\theta = \arg(t)$ and t is the total transmission coefficient of the entire system. It is observed that the phase shift in the transparency window is deeper when ε_{d} is close to 1 and 4; this is because the resonance condition is nearly satisfied here and therefore possesses a deep phase dispersion, the details of which will be discussed in a later section. This gives further support to the fact that the PIT effect is realized in a constant separation. In figures 2(hi)–($h$iii), we show the average magnetic field distributions at 723, 736.4 and 747 nm for transmission spectra in figure 2(a). The appearance of a transmission peak at 736.4 nm is attributed to the Fabry–Perot resonance between the two ring resonators. Therefore, the incident light can propagate through the waveguide system uninhibitedly at wavelength 736.4 nm, while being stored in ring resonators and reflected back at the other two wavelengths.

The influence of wavelength detuning $\Delta\lambda$ on transmission spectra is considered to get a further verification of the obtained TMM. Here, we assume ε_{d} = 1 for brevity. Radius R_1 = 179, 178, 177, 176 nm and R_2 = 170, 171, 172, 173 nm for figures 3(a)–(d), respectively; d is chosen to be 200 nm for a non-resonance situation; other parameters remain the same as those in figure 1(a). We can also get d = 240 nm for resonance, which can be calculated through the relation that propagation phase φ is equal to an integral multiple of π. The QFs for the theoretical fitting in figures 3(a)–(d) are given as $Q_{\mathrm{t}1(2)}$ = 46.9 (110), 56 (104.2), 50.8 (91.7) and 53.1 (82.4) for ring 1 (2), respectively. Here we discuss the impact of

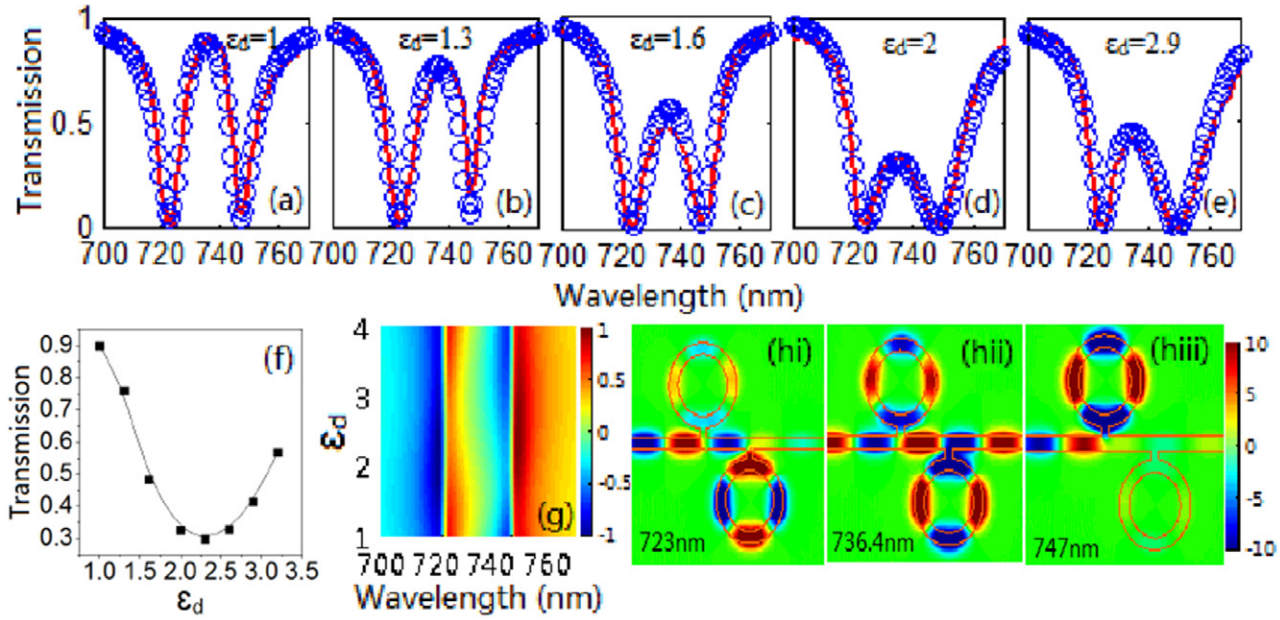

Figure 2. Transmission spectra of the structure in figure 1(*a*) using FDTD (red line) and TMM (blue circles) for $R_1 = 174$ nm, $R_2 = 171$ nm and $d = 250$ nm with (*a*)$\varepsilon_d = 1$, (*b*)$\varepsilon_d = 1.3$, (*c*)$\varepsilon_d = 1.6$, (*d*)$\varepsilon_d = 2.0$, (*e*)$\varepsilon_d = 2.9$. (*f*) Relation between transmission maximum in the transparency window and ε_d; (*g*) evolution of the transmission phase shift θ with ε_d. (*h*i)–(*h*iii) Average magnetic field distributions of the transmission dips and peak in (*a*).

$\Delta\lambda$ in the non-resonance condition to give a comparison to that when the resonance condition is satisfied, which has been reported [15]. A nearly asymmetric line shape can be observed in figures 3(*a*)–(*d*), which is attributed to the coupling in non-resonance, and the transparency window broadens as $\Delta\lambda$ increases. To study the slow-light effect, we then investigate the phase and group dispersion in the transparency window. A structure with $R_1 = 176$ nm and $R_2 = 173$ nm is taken as an example, shown in figure 3(*e*). The group index n_g is calculated through the formula $n_g = c/v_g = c/H\tau_g = c/H(\mathrm{d}\theta(\omega)/\mathrm{d}\omega)$, where v_g is the group velocity, τ_g is the delay time, the phase shift $\theta(\omega)$ is a function of angular frequency ω and $H = 900$ nm is the length of the plasmonic system. When $d = 240$ nm the phase shift in the transparency window is deeper and leads to a maximum $n_g \sim 22$, while it is shallower when $d = 200$ nm and therefore leads to a smaller $n_g \sim 15$. This can be regarded as support for the discussion in the previous section. The negative n_g near the transparency window, corresponding to a negative τ_g, which reveals a fast light in this system, is also observed [19, 26]. In addition, the relation between n_g and radius detuning ΔR is also plotted as figure 3(*f*). For both $d = 200$ and 240 nm, n_g show a decreasing trend as ΔR increases. Moreover, a higher n_g can be obtained when the resonance condition is satisfied (shown as black squares). Here an interesting phenomenon is observed: that the difference of n_g for each ΔR gets smaller as ΔR increases, which may be attributed to the deep dispersion in a small detuning resonator-coupled system.

3.2. Tunable dispersion based on PIT in periodic coupled MDM system

In this section, we discuss the dispersion relation of a periodic system with unit cell mentioned above and period p, shown in figure 1(*b*); $A_{\pm 2'}$ and $A_{\pm 3'}$ are used here for distinction. For a single unit cell, all parameters remain the same in figure 3(*d*) except for $d = 240$ nm as a special case, which makes the propagation term exp(*h*) equal to unity for brevity in the next deduction and guarantees a deep dispersion. Assuming that no propagation loss exists between unit cells, only the phase difference φ' is considered, therefore the related TMM for figure 1(*b*) can be given as

$$\begin{pmatrix} 0 & \mathrm{e}^{\mathrm{i}\varphi'} \\ \mathrm{e}^{-\mathrm{i}\varphi'} & 0 \end{pmatrix} \begin{pmatrix} A_{+2'} \\ A_{-2'} \end{pmatrix} = \begin{pmatrix} A_{+3'} \\ A_{-3'} \end{pmatrix},$$
$$\text{where } \varphi' = \frac{2\pi \mathrm{Re}(n_{\mathrm{eff}})(p - d - w')}{\lambda} \tag{9}$$

and

$$\begin{pmatrix} -\dfrac{r_1 r_2}{t_1 t_2}\mathrm{e}^{\mathrm{i}\varphi'} + \left(\dfrac{r_1}{t_1}+1\right)\left(\dfrac{r_2}{t_2}+1\right)\mathrm{e}^{\mathrm{i}\varphi'} & \dfrac{r_2}{t_1 t_2}\mathrm{e}^{\mathrm{i}\varphi'} + \dfrac{r_1}{t_1}\left(\dfrac{r_2}{t_2}+1\right)\mathrm{e}^{\mathrm{i}\varphi'} \\ -\dfrac{r_1}{t_1 t_2}\mathrm{e}^{-\mathrm{i}\varphi'} - \dfrac{r_2}{t_2}\left(\dfrac{r_1}{t_1}+1\right)\mathrm{e}^{-\mathrm{i}\varphi'} & \dfrac{1}{t_1 t_2}\mathrm{e}^{-\mathrm{i}\varphi'} - \dfrac{r_1 r_2}{t_1 t_2}\mathrm{e}^{-\mathrm{i}\varphi'} \end{pmatrix} \times \begin{pmatrix} A_{+1} \\ A_{-1} \end{pmatrix} = \mathrm{M}\begin{pmatrix} A_{+1} \\ A_{-1} \end{pmatrix} = \begin{pmatrix} A_{+3'} \\ A_{-3'} \end{pmatrix}. \tag{10}$$

Based on the Bloch theory, which is widely listed in the literature [27, 28], the relation of input and output amplitudes can be expressed as

$$\begin{pmatrix} \mathrm{e}^{-\mathrm{i}pK} & 0 \\ 0 & \mathrm{e}^{-\mathrm{i}pK} \end{pmatrix} \begin{pmatrix} A_{+1} \\ A_{-1} \end{pmatrix} = \mathrm{P}\begin{pmatrix} A_{+1} \\ A_{-1} \end{pmatrix} = \begin{pmatrix} A_{+3'} \\ A_{-3'} \end{pmatrix}, \tag{11}$$

where $K = \alpha + \mathrm{i}\beta$ is the Bloch wave vector. In order to calculate the propagation constant β for the periodic structure, the corresponding determinant should satisfy the formula that

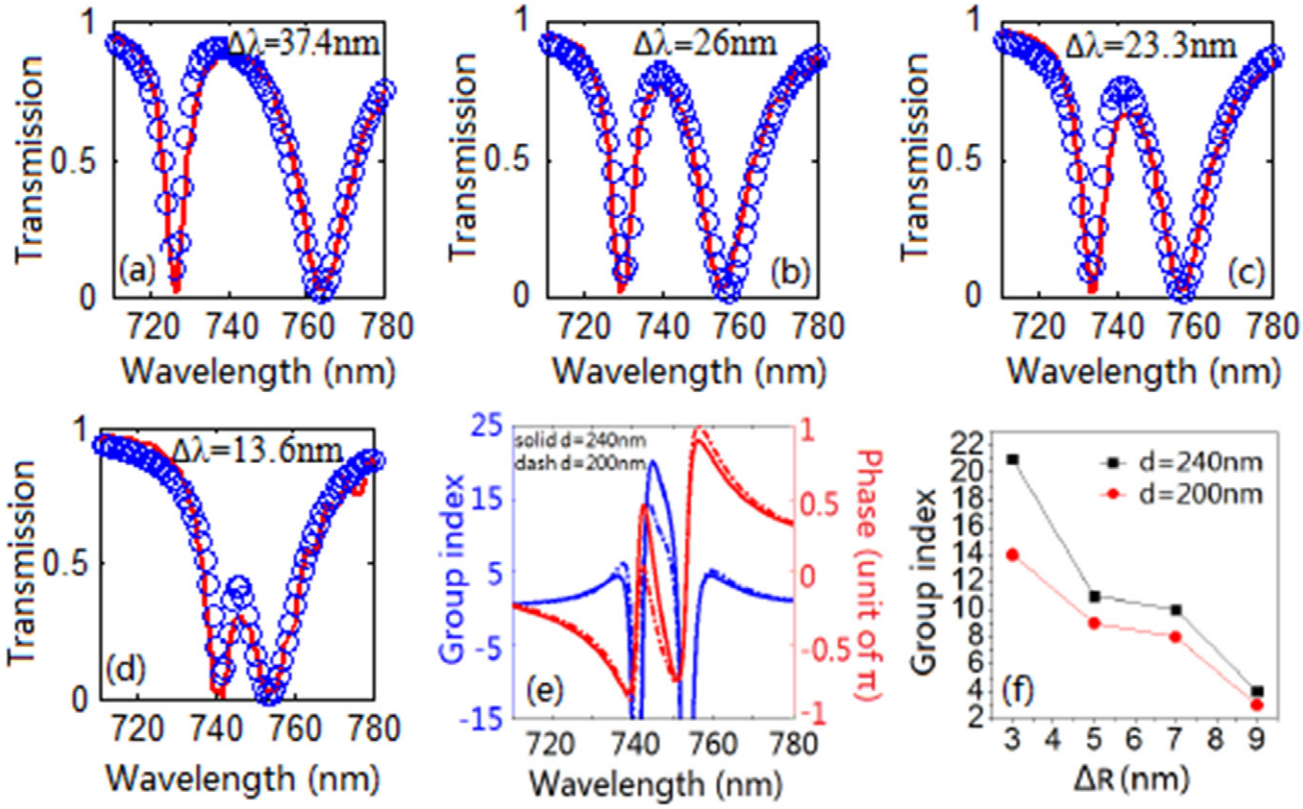

Figure 3. Transmission spectra of the structure in figure 1(*a*) using FDTD (red line) and TMM (blue circles) for $d = 200$ nm with varied wavelength detuning $\Delta\lambda$: (*a*) 37.4 nm, (*b*) 26 nm, (*c*) 23.3 nm, (*d*) 13.6 nm. (*e*) Phase (red) and group dispersion (blue) in the transparency window with $R_1 = 176$ nm and $R_2 = 173$ nm for $d = 200$ nm and 240 nm, respectively; (*f*) the relation between n_g and radius detuning ΔR.

$|\mathrm{M} - \mathrm{IP}| = 0$ [29], where I represents the unit matrix. Since matrices M and P are given in equations (10) and (11), the dispersion relation of the whole system can be derived as

$$\exp(-2\mathrm{i}pK) - (B+E)\exp(-\mathrm{i}pK) + (BE - CD) = 0, \tag{12}$$

where $B = -r_1r_2/(t_1t_2)\mathrm{e}^{\mathrm{i}\varphi'} + (r_1/t_1+1)(r_2/t_2+1)\mathrm{e}^{\mathrm{i}\varphi'}$, $C = r_2/(t_1t_2)\mathrm{e}^{\mathrm{i}\varphi'} + (r_1/t_1)(r_2/t_2+1)\mathrm{e}^{\mathrm{i}\varphi'}$, $D = -r_1/(t_1t_2)\mathrm{e}^{-\mathrm{i}\varphi'} - (r_2/t_2)(r_1/t_1+1)\mathrm{e}^{-\mathrm{i}\varphi'}$, $E = 1/(t_1t_2)\mathrm{e}^{-\mathrm{i}\varphi'} - (r_1r_2)/(t_1t_2)\mathrm{e}^{-\mathrm{i}\varphi'}$.

The dispersion relation of the system with $p = 785$ nm (790 nm) is plotted as the red (blue) line in figure 4(*a*). Here the frequency unit THz for the vertical axis is used in the following discussion for clarity. The band between 401 and 404 THz corresponds to a mode with slow group velocity $v_g = \partial\omega/\partial\beta$. So we can approximately consider that the slope at a point on the curve represents the corresponding v_g at this frequency. Then we infer that the group index n_g around the transparency peak at 402.5 THz (~745.4 nm) for $p = 785$ nm is larger than that for $p = 800$ nm due to the smaller slope. This deduction is confirmed by figure 4(*b*) (red circles), where n_g is presented as a function of period p. n_g is calculated to be 18 for $p = 785$ nm while 12 for $p = 800$ nm at the peak. The slow-light effect for even smaller p is also analysed. As p decreases, the group index increases inversely and reaches 21 when $p = 740$ nm. The observation here is different from that in [12], where the group index for a certain frequency decreases with decreasing p. This can be attributed to the difference in coupling mechanism, where direct coupling is noticed in that system while only indirect coupling is considered here. In addition, the maximum n_g in the transparency window (TW) with varied p is plotted in figure 4(*b*) (black squares) as well. We find that n_g shows a similar increase as p decreases but we get a higher value than that at the peak and a high group index ~51 is achieved when $p = 740$ nm. This gives an understanding that p can be effective in tuning the slow-light effect in this system. Finally, we briefly investigate the impact that the QF of the resonator has on the dispersion relation when p keeps constant and is chosen to be 785 nm. As the QF Q_{t1} increases from 53.1 to 143.1 with a step of 30, the dispersion curve is displayed as figure 4(*c*). We can see that the frequency has an almost linear relationship with the propagation constant β in the slow-light bands. For a given frequency of 402.5 THz, the slope shows a distinct increasing trend as Q_{t1} increases. The calculated n_g for different Q_{t1} values is plotted as the inset in figure 4(*c*), and the corresponding n_g decreases from 18 to 12 as Q_{t1} increases from 53.1 to 143.1. The situation for Q_{t2} is not discussed here due to the similar results. So far, we have presented a convenient way to adjust the n_g for a given frequency by changing the QF of resonators and period p in a periodic waveguide system.

4. Conclusions

In conclusion, a theoretical and numerical investigation has been made of the PIT effect in a dual-ring resonator-coupled

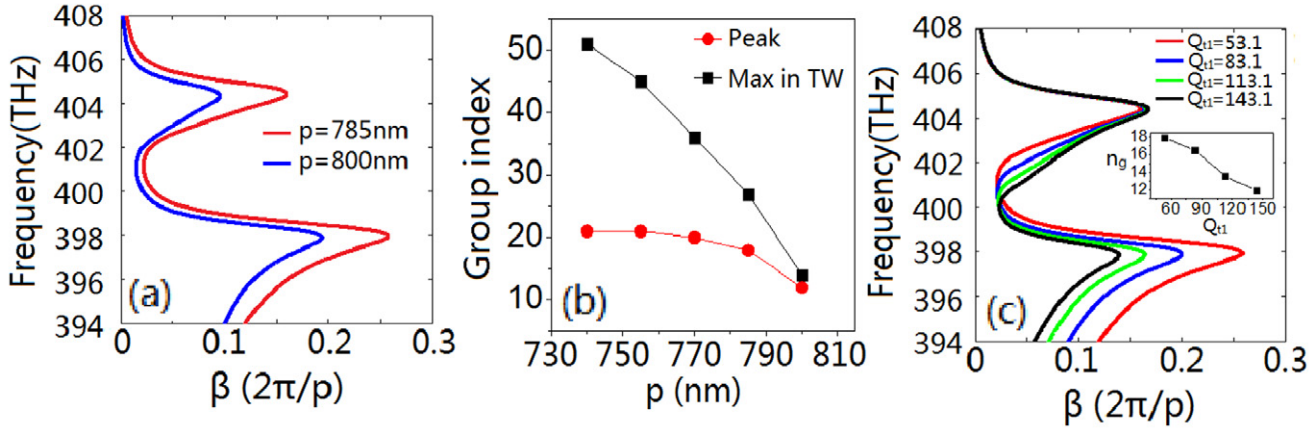

Figure 4. (*a*) Dispersion relation of the system with $p = 785$ nm (red) and 790 nm (blue); (*b*) n_g as a function of period p; (*c*) dispersion curves when QF Q_{t1} increases from 53.1 to 140.1 with a step of 30.

MDM waveguide system. The introduced TMM shows good agreement in analysing the transmission and dispersion property in the transparency window. According to the novel design, a tunable PIT effect is realized in a constant separation design. The phase and group dispersion relations are proved to be deeper and higher in the resonance than in the non-resonance condition. Finally, the derived propagation constant for the periodic system revealed that the group index in the transparency window of the proposed structure can be easily tuned by period p, which provides a new understanding and a group index ~51 is achieved. We also found that the quality factor of resonators can be effective in adjusting the dispersion relation. This proposed configuration can be helpful in fundamental research and applications for integrated plasmonic devices.

Acknowledgments

This work was funded by the Fundamental Research Funds for the Central Universities of Central South University under grants No 72150050429 and No 2012zzts007, the Research Fund for the Doctoral Program of Higher Education of China under Grant No 20100162110068, and the National Natural Science Foundations of China under Grant No 61275174.

References

[1] Fleischhauer M, Imamoglu A and Marangos J P 2005 *Rev. Mod. Phys.* **77** 633
[2] Harris S E 1997 *Phys. Today* **50** 36
[3] Zhu L, Meng F Y, Fu J H and Wu Q 2012 *J. Phys. D: Appl. Phys.* **45** 445105
[4] Lu X Q, Shi J H, Liu R and Guan C Y 2012 *Opt. Express* **20** 17581
[5] Dong Z G, Liu H, Xu M X, Li T, Wang S M, Zhu S N and Zhang X 2010 *Opt. Express* **18** 18229
[6] Zhou J H, Mu D, Yang J H, Han W B and Di X 2011 *Opt. Express* **19** 4856
[7] Tang B, Dai L and Jiang C 2011 *Opt. Express* **19** 628
[8] Min C J and Veronis G 2009 *Opt. Express* **17** 10757
[9] Huang Y, Min C J and Veronis G 2012 *Opt. Express* **20** 22233
[10] Han Z H and Bozhevolnyi S I 2011 *Opt. Express* **19** 3251
[11] Cao G T, Li H J, Zhan S P, Xu H Q, Liu Z M, He Z H and Wang Y 2013 *Opt. Express* **21** 9198
[12] Huang Y, Min C J and Veronis G 2011 *Appl. Phys. Lett.* **99** 143117
[13] Wang G X, Lu H and Liu X M 2012 *Opt. Express* **20** 20902
[14] Lu H, Liu X M and Mao D 2012 *Phys. Rev.* A **85** 053803
[15] Kekatpure R D, Barnard E S, Cai W S and Brongersma M L 2010 *Phys. Rev. Lett.* **104** 243902
[16] Kocabas S E, Veronis G, Miller D A B and Fan S H 2008 *IEEE J. Quantum Electron.* **14** 1462
[17] Pannipitiya A, Rukhlenko I D, Premaratne M, Hattori H T and Agrawal G P 2010 *Opt. Express* **18** 6191
[18] Han Z, Van V, Herman W N and Ho P T 2009 *Opt. Express* **17** 12678
[19] Li Q, Wang T, Su Y K, Yan M and Qiu M 2010 *Opt. Express* **18** 8367
[20] Yariv A 1973 *IEEE J. Quantum Electron.* **9** 919
[21] Zhang Q, Huang X G, Lin X S, Tao J and Jin X P 2009 *Opt. Express* **17** 7549
[22] Park J, Kim H and Lee B 2008 *Opt. Express* **16** 413
[23] Taflove A and Hagness S C 2005 *Computational Electrodynamics*: *The Finite-Difference Time-Domain Method* 3rd edn (Boston, MA: Artech House)
[24] Han Z H 2010 *Photon. Nanostruct.* **8** 172
[25] Bozhevolnyi S I and Jung J 2008 *Opt. Express* **16** 2676
[26] Totsuka K, Kobayashi N and Tomita M 2007 *Phys. Rev. Lett.* **98** 213904
[27] Maes B, Bienstman P and Baets R 2005 *J. Opt. Soc. Am.* B **22** 1778
[28] Poon J K S, Scheuer J, Mookherjea S, Paloczi G T, Huang Y and Yariv A 2004 *Opt. Express* **12** 90
[29] Lin X S and Yan J H 2009 *Opt. Commun.* **282** 3081